Exact Vlasov-Maxwell equilibria for asymmetric current sheets

AGU PUBLICATIONS

Geophysical Research Letters

RESEARCH LETTER
10.1002/2017GL074168

Key Points:
- New exact Vlasov-Maxwell equilibria for 1D asymmetric current sheets
- Written as a combination of four shifted Maxwellian distribution functions
- Self-consistent with asymmetric magnetic field, temperature, density, and pressure profiles

Correspondence to:
O. Allanson,
oliver.allanson@st-andrews.ac.uk

Citation:
Allanson, O., F. Wilson, T. Neukirch, Y.-H. Liu, and J. D. B. Hodgson (2017), Exact Vlasov-Maxwell equilibria for asymmetric current sheets, *Geophys. Res. Lett.*, *44*, doi:10.1002/2017GL074168.

Received 15 MAY 2017
Accepted 6 AUG 2017
Accepted article online 14 AUG 2017

Exact Vlasov-Maxwell equilibria for asymmetric current sheets

O. Allanson[1,2], F. Wilson[1], T. Neukirch[1], Y.-H. Liu[3], and J. D. B. Hodgson[1]

[1]Solar and Magnetospheric Theory Group, School of Mathematics and Statistics, University of St Andrews, Saint Andrews, UK, [2]Space and Atmospheric Electricity Group, Department of Meteorology, University of Reading, Reading, UK, [3]NASA-Goddard Space Flight Center, Greenbelt, Maryland, USA

Abstract The NASA Magnetospheric Multiscale mission has made in situ diffusion region and kinetic-scale resolution measurements of asymmetric magnetic reconnection for the first time, in the Earth's magnetopause. The principal theoretical tool currently used to model collisionless asymmetric reconnection is particle-in-cell simulations. Many particle-in-cell simulations of asymmetric collisionless reconnection start from an asymmetric Harris-type magnetic field but with distribution functions that are not exact equilibrium solutions of the Vlasov equation. We present new and exact equilibrium solutions of the Vlasov-Maxwell system that are self-consistent with one-dimensional asymmetric current sheets, with an asymmetric Harris-type magnetic field profile, plus a constant nonzero guide field. The distribution functions can be represented as a combination of four shifted Maxwellian distribution functions. This equilibrium describes a magnetic field configuration with more freedom than the previously known exact solution and has different bulk flow properties.

Plain Language Summary Magnetic reconnection is a fundamental phenomenon in space science and is currently a subject of intense study. During a reconnection event, stored energy that had been bound up in stressed electromagnetic fields is released in the form of heat and the kinetic energy of particles. The NASA MMS mission is currently making measurements of these phenomena in the Earth's Magnetosphere, with unprecedented levels of accuracy and resolution. Our work presents a theoretical model of a structure in space known as an asymmetric current sheet such as the MMS mission encounters during a reconnection event. The model can be implemented into computer simulations, with which to compare to the results from MMS satellite data. This will help us understand the fundamental physics of asymmetric magnetic reconnection.

1. Introduction

The formation of current sheets is ubiquitous in plasmas. These current sheets form between plasmas of different origins that encounter each other, such as at Earth's magnetopause between the magnetosheath and magnetospheric plasmas [*Dungey*, 1961; *Phan and Paschmann*, 1996]; or they develop spontaneously in magnetic fields that are subjected to random external drivings [*Parker*, 1994], such as in the solar corona region. Under most circumstances, the plasma conditions on either side of the current sheet can be different, e.g., the magnetic field strength and orientation. Such current sheets are dubbed asymmetric. Asymmetric current sheets are also observed at Earth's magnetotail [*Øieroset et al.*, 2004], in the solar wind [*Gosling et al.*, 2006], between solar flux tubes [*Linton*, 2006; *Murphy et al.*, 2012; *Zhu et al.*, 2015], in turbulent plasmas [*Servidio et al.*, 2009; *Karimabadi et al.*, 2013], and inside tokamaks [*Kadomtsev*, 1975].

As per Poynting's theorem [*Poynting*, 1884; *Birn and Hesse*, 2010], these intense current sheets are ideal locations for magnetic energy conversion and dissipation [*Zenitani et al.*, 2011]. The dominant mechanisms that release the free energy include magnetic reconnection, and various plasma instabilities. The asymmetric feature has now been included in modeling the reconnection rate [*Cassak and Shay*, 2007], the development of the lower hybrid instability [*Roytershteyn et al.*, 2012] and the suppression of reconnection at Earth's magnetopause [*Swisdak et al.*, 2003; *Phan et al.*, 2013; *Trenchi et al.*, 2015; *Liu and Hesse*, 2016]. The physics in the linear stage could affect the dynamical evolution of the current sheets [*Dargent et al.*, 2016]. Thus, developing an exact Vlasov equilibrium for the current sheet is important, but it is challenging. The well-known solution of the symmetric Harris sheet [*Harris*, 1962] has been extended to the relativistic regime [*Hoh*, 1966],

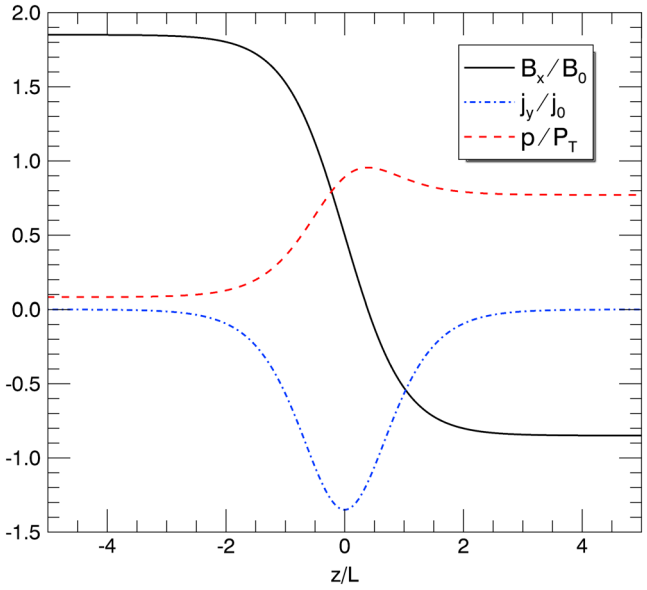

Figure 1. Normalized magnetic field $\tilde{B}_x$, current density $\tilde{j}_y$, and scalar pressure $\tilde{p}$ for *Parameter Set One*.

the Kappa distribution [*Fu and Hau*, 2005], and later the force-free limit [*Harrison and Neukirch*, 2009a; *Wilson and Neukirch*, 2011; *Stark and Neukirch*, 2012; *Abraham-Shrauner*, 2013; *Allanson et al.*, 2015; *Kolotkov et al.*, 2015; *Allanson et al.*, 2016]. In this letter, we present a new exact Vlasov-Maxwell equilibrium solution for asymmetric current sheets.

The intention of the exact solution that we present in this paper is to represent a step forward in the analytical modeling of asymmetric Vlasov-Maxwell equilibria, which is of particular relevance to particle-in-cell (PIC) simulations and analysis using kinetic theory. Inevitably, working within the confines of an exact model does imply that we cannot accurately represent all desired features of the magnetopause current sheet system, and some of these restrictions will be discussed.

1.1. The Current Sheet Equilibrium

The specific magnetic field profile that we consider is a one-dimensional (1D) current sheet, composed of an 'asymmetric Harris sheet' with a constant guide field, such as that first used in analytical study of the tearing mode at the dayside Magnetopause in *Quest and Coroniti* [1981]. In *mks* units and $(\hat{x},\hat{y},\hat{z}) \sim (\hat{L},\hat{M},\hat{N})$ coordinates [e.g., see *Hapgood*, 1992], the vector potential, magnetic field and current density for the 'asymmetric Harris sheet plus guide' (AH+G) model can be written

$$\begin{aligned} \boldsymbol{A}(\tilde{z}) &= B_0 L(\, C_3\tilde{z},\, -C_1\tilde{z} - C_2 \ln\cosh\tilde{z},\, 0), \\ \nabla\times\boldsymbol{A} = \boldsymbol{B}(\tilde{z}) &= B_0(\, C_1 + C_2\tanh\tilde{z},\, C_3,\, 0), \end{aligned} \tag{1}$$

$$\frac{1}{\mu_0}\nabla\times\boldsymbol{B} = \boldsymbol{j}(\tilde{z}) = \frac{B_0}{\mu_0 L}(\, 0,\, C_2\,\mathrm{sech}^2\tilde{z},\, 0), \tag{2}$$

respectively, with μ_0 the magnetic permeability in vacuo; C_1, C_2, and $C_3 \neq 0$ dimensionless constants; and B_0 and L dimensional constants that normalize the vector potential ($\boldsymbol{A} = B_0 L\tilde{\boldsymbol{A}}$), magnetic field ($\boldsymbol{B} = B_0\tilde{\boldsymbol{B}}$), current density ($\boldsymbol{j} = j_0\tilde{\boldsymbol{j}}$), and z ($z = L\tilde{z}$), with $j_0 = B_0/(\mu_0 L)$.

The fluid equilibrium for the AH+G current sheet is maintained by the gradient of a scalar pressure, $p = p(z)$, according to $\nabla p = \boldsymbol{j}\times\boldsymbol{B}$ and $d/dz[p + B^2/(2\mu_0)] = 0$. The scalar pressure in force balance with the AH+G field is given by

$$p(\tilde{z}) = P_T - \frac{B_0^2}{2\mu_0}\left(C_1^2 + 2C_1C_2\tanh\tilde{z} + C_2^2\tanh^2\tilde{z} + C_3^2\right), \tag{3}$$

for P_T the total pressure (magnetic plus thermal), and $p(z) > 0$ for $C_1^2 + 2|C_1C_2| + C_2^2 + C_3^2 < 2\mu_0 P_T/B_0^2$. Example profiles of $\tilde{B}_x, \tilde{j}_y$, and $\tilde{p}(\tilde{z}) = p/P_T$ are plotted in Figure 1 for parameter values $C_1 = 0.5$, $C_2 = -1.35$, $C_3 \approx -0.42$, and $P_T \approx 3.92B_0^2/(2\mu_0)$, and hereafter referred to as *Parameter Set One*. For *Parameter Set One*, the left- and right-hand sides of the plot could represent the magnetosphere and magnetosheath, respectively, while the central current sheet is in the magnetopause (see Figure 2 for a representative diagram of the equilibrium configuration). *Parameter Set One* corresponds to magnetic field asymmetry, total magnetic shear, and number density/scalar pressure asymmetries of

$$B_{\mathrm{ratio}} = \frac{|\boldsymbol{B}_{\mathrm{sphere}}|}{|\boldsymbol{B}_{\mathrm{sheath}}|} = 2, \quad \phi_{B,\mathrm{shear}} = \cos^{-1}\left(\hat{\boldsymbol{b}}_{\mathrm{sphere}}\cdot\hat{\boldsymbol{b}}_{\mathrm{sheath}}\right) \approx 140^\circ$$

$$n_{\mathrm{ratio}} = \frac{n_{\mathrm{sheath}}}{n_{\mathrm{sphere}}} = p_{\mathrm{ratio}} = \frac{p_{\mathrm{sheath}}}{p_{\mathrm{sphere}}} \approx 9.50,$$

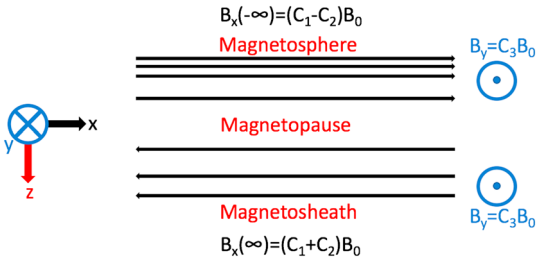

Figure 2. A representative diagram of the equilibrium magnetic field, for $C_1 + C_2 < 0$, $C_1 - C_2 > 0$ and $C_3 < 0$.

with $\hat{\boldsymbol{b}}$ the magnetic field unit vector, the *sheath*/*sphere* subscripts denoting $z = \infty, -\infty$, respectively. These asymmetries show positive similarities with certain magnetopause properties, given typical magnetopause conditions [e.g., see *Burch et al.*, 2016; *Hesse et al.*, 2016]. We stress that these asymmetries relate to a particular selection of parameters, which are chosen to demonstrate an example of the types of asymmetric conditions that the distribution function (DF) can support.

The ratio of the number densities was derived using a relation, $p(\tilde{z}) = Cn(\tilde{z})$, for C a constant. This "fluid" relation is valid even for the Vlasov model that we shall derive, but this does not mean that the "kinetic temperature" is constant and merits the following discussion. The macroscopic force balance self-consistent with a quasineutral Vlasov equilibrium is maintained by the divergence of a rank-2 pressure tensor, $P_{ij} = P_{ij}(A_x(z), A_y(z))$ [e.g., see *Channell*, 1976; *Mynick et al.*, 1979; *Schindler*, 2007], according to $\nabla \cdot \boldsymbol{P} = \boldsymbol{j} \times \boldsymbol{B}$. Hence, $p = nk_BT$ is in principle an approximation to the kinetic physics, with the pressure and temperature properly defined by rank-2 pressure tensors. However, in our geometry, the scalar pressure that maintains fluid equilibrium is identified with the pressure tensor component that is self-consistent with a kinetic equilibrium, according to $p = P_{zz}$ [e.g., see *Harrison and Neukirch*, 2009a], giving

$$\frac{d}{dz}\left(P_{zz} + \frac{B^2}{2\mu_0}\right) = 0. \tag{4}$$

Note that P_{zz} is not the only nonzero component of P_{ij}, but it is the only component that plays a role in the force balance of the equilibrium. It can be shown [*Channell*, 1976] that for 1D Vlasov-Maxwell equilibria like that considered in this paper, $p = P_{zz} = Cn$ holds, and so our expression for n_{ratio} is correct for both the fluid and kinetic approaches. In section 2.2 we shall use other components of P_{ij} to define the kinetic temperature, which is asymmetric, as plotted in Figure 5.

The AH+G magnetic field is very similar to a magnetic field introduced in the Appendix of *Alpers* [1969], in a rotated coordinate system: the AH+G field defined in equation (1) reproduces the "Alpers magnetic field" under a rotation $\tan\theta = C_1/C_3$. However, the Alpers magnetic field has one fewer degree of freedom (i.e., an extra constraint on C_1, C_2, and C_3).

1.2. Nonequilibrium Initial Conditions for PIC Simulations

In the effort to model asymmetric magnetopause reconnection, fields such as the Alpers and AH+G models, and variations that could involve a "double" current sheet structure and/or no guide field have been used in PIC simulations in, e.g., *Swisdak et al.* [2003], *Pritchett* [2008], *Huang et al.* [2008], *Malakit et al.* [2010], *Wang et al.* [2013], *Aunai et al.* [2013], *Hesse et al.* [2013], *Hesse et al.* [2014], *Dargent et al.* [2016], and *Liu and Hesse* [2016]. All of these studies except that of *Dargent et al.* [2016] have used "flow-shifted" Maxwellian DFs as initial conditions

$$f_{\text{Maxw},s}(z, \boldsymbol{v}) = \frac{n(z)}{\left(\sqrt{2\pi}v_{th,s}\right)^3} \exp\left[\frac{\left(\boldsymbol{v} - \boldsymbol{V}_s(z)\right)^2}{2v_{th,s}^2}\right], \tag{5}$$

with $v_{th,s}$ a characteristic value of the thermal velocity of species s, $\boldsymbol{V}_s$ the bulk velocity of species s, and $n(z)$ the number density. These DFs can reproduce the same moments $(n(z), \boldsymbol{V}_s(z), p(z))$ necessary for a quasineutral fluid equilibrium.

Despite the fact that the DF, $f_{\text{Maxw},s}$, in equation (5) reproduces the desired moments, it is not an exact solution of the Vlasov equation and hence does not describe a kinetic equilibrium. As explained in *Aunai et al.* [2013] on the subject of particle-in-cell (PIC) simulations, the fluid equilibrium characterized by a flow-shifted Maxwellian can evolve to a quasi steady state "with an internal structure very different from the prescribed one," and as demonstrated in *Pritchett* [2008], undesired electric fields, E_z, "coherent bulk oscillations" and other perturbations may form.

The main aim of this paper is to calculate exact solutions of the equilibrium Vlasov-Mawell equations consistent with the AH+G magnetic field in equation (1), in order to circumvent the need to use nonequilibrium kinetic DFs of the form in equation (5) as initial conditions in collisionless PIC simulations of asymmetric reconnection.

1.3. Two Prior Vlasov-Maxwell Equilibria for Asymmetric Current Sheets

In the Appendix to *Alpers* [1969], a DF is derived that is consistent with the Alpers magnetic field (as described in section 1.1). As is necessary for consistency between the microscopic and macroscopic descriptions, the Alpers DF is self-consistent with the prescribed magnetic field; i.e., the sum of the individual species (kinetic) currents are equal to the current prescribed by Ampère's law, i.e., $\sum_s \boldsymbol{j}_s = \boldsymbol{j} = \nabla \times \boldsymbol{B}/\mu_0$. However, the $\boldsymbol{j}_s$ are nonzero at $z = +\infty$ (in our coordinates), i.e., the magnetosheath side. In contrast, equation (2) shows that the macroscopic current densities vanish as $z \to \pm\infty$; i.e., the Alpers DF gives species currents $\boldsymbol{j}_s$ that are not proportional to the macroscopic current $\boldsymbol{j}$. That is to say that there is finite ion and electron mass flow at infinity. This could be appropriate if one wishes to consider a larger scale/global magnetopause model that includes flows at the boundary corresponding to the magnetosheath, for example, but it might not be appropriate if one wishes to consider the domain as a "patch," representing a current sheet structure locally (while formally speaking, the spatial domain in our model is infinite; this is not necessarily intended to reproduce the entire spatial domain of the solar wind-magnetosheath-magnetopause-magnetosphere system). The nonvanishing of the individual species bulk flows at the boundaries in the Alpers equilibrium are also inconsistent with most of the initial conditions of typical PIC simulations of asymmetric reconnection, viz., in the absence of an exact Vlasov equilibrium the simulations are typically initiated with a shifted Maxwellian consistent with zero species flow at the boundary. The DF that we derive shall be consistent macroscopically with an equilibrium for which there are no mass flows at infinity and is self-consistent with a magnetic field that has more degrees of freedom than that in *Alpers* [1969].

The second relevant work is that of *Belmont et al.* [2012], in which "semianalytic" Vlasov-Maxwell equilibria are found numerically. The magnetic field in that paper is actually a symmetric Harris sheet without guide field, i.e., $C_1 = C_3 = 0$, but with asymmetric profiles of the density, pressure, and temperature. The DFs calculated therein are not found using a typical constants of motion approach as is to be used in this paper. Instead, they are found by considering ion DFs, such that when expressed in terms of the motion invariants, are double-valued functions. The "semianalytic" DF that is derived by *Belmont et al.* [2012] has been used as the initial condition for PIC simulations in *Dargent et al.* [2016]. The model was generalized by *Dorville et al.* [2015] to include a magnetic field profile similar to the force-free Harris sheet [*Harrison and Neukirch*, 2009a], and also an electric field profile.

2. New Vlasov-Maxwell Equilibrium for Asymmetric Current Sheets

2.1. Channell's Method

The AH+G equilibrium defined by equations (1) and (4) is translationally invariant in the xy plane, giving rise to two conserved canonical momenta for particles of species s, $p_{xs} = m_s v_x + q_s A_x$, $p_{ys} = m_s v_y + q_s A_y$. Because we are considering an equilibrium, the particle Hamiltonian of species s is also conserved, $H_s = m_s v^2/2 + q_s \phi$, for ϕ the electrostatic potential. Jeans' theorem implies that one can always solve the Vlasov equation by choosing f_s to be a function of known constants of motion [*Jeans*, 1915; *Lynden-Bell*, 1962], and the solution will be physically meaningful provided $f_s \geq 0$ and velocity-space moments of all order exist [*Schindler*, 2007]. Using this fact, and assumptions common to much theoretical work on 1D translationally invariant Vlasov-Maxwell equilibria [e.g., see *Alpers*, 1969; *Channell*, 1976; *Schindler*, 2007; *Harrison and Neukirch*, 2009a; *Wilson and Neukirch*, 2011; *Abraham-Shrauner*, 2013; *Kolotkov et al.*, 2015; *Allanson et al.*, 2015, 2016], we assume $\phi = 0$ (strict neutrality) and that

$$f_s(H_s, p_{xs}, p_{ys}) = \frac{n_{0s}}{(\sqrt{2\pi} v_{th,s})^3} e^{-\beta_s H_s} g_s(p_{xs}, p_{ys}), \tag{6}$$

for n_{0s} a constant with dimensions of number density, $\beta_s = 1/(m_s v_{th,s}^2)$, m_s the mass and g_s an unknown function of the canonical momenta for particle species s, which is yet to be determined. Calculating self-consistent g_s functions (and hence Vlasov equilibrium DFs) for a given macroscopic equilibrium is an example of the "inverse problem in collisionless equilibria" [e.g., see *Channell*, 1976; *Allanson et al.*, 2016], for which there is not necessarily a guaranteed exact solution. The method that we shall use is known as "Channell's method"

[*Channell*, 1976] which is used in many of the works listed above and has been somewhat generalized in *Mottez* [2003]. We note that a treatment of this inverse problem is given in *Alpers* [1969] that is very similar to that of Channell. The major benefit of using Channell's method for this problem is that we obtain an exact solution that is readily implementable, but one downside is that the asymmetry of the number density is directly tied to that of the magnetic field; i.e., there can be no asymmetry in the density profile when $C_1 = 0$. This is in contrast to the numerical methods used by *Belmont et al.* [2012] and *Dorville et al.* [2015].

The method rests on calculating a functional form of $P_{zz}(A_x, A_y)$ that "reproduces" the scalar pressure of equation (3) as a function of z, i.e., $P_{zz}(A_x, A_y)(z) = p(z)$, but also that satisfies $\partial P_{zz}/\partial \boldsymbol{A} = \boldsymbol{j}(z)$ (for fuller details on the background theory of this first and crucial step, see, e.g., *Mynick et al.* [1979], *Schindler* [2007], and *Harrison and Neukirch* [2009b]). There could in principle be infinitely many functions $P_{zz}(A_x, A_y)$ that satisfy both the criteria necessary for Channell's method; however, we shall choose a specific $P_{zz}(A_x, A_y)$ which allows us to make analytical progress.

Similar to the procedure in *Alpers* [1969], by substituting linear combinations of two distinct representations of $\tanh\tilde{z}(A_x, A_y)$,

$$\tanh\tilde{z} = 1 - e^{-\tilde{z}}\mathrm{sech}\tilde{z} = 1 - e^{\frac{C_1-C_2}{C_2C_3}\tilde{A}_x}e^{\frac{1}{C_2}\tilde{A}_y},$$
$$\tanh\tilde{z} = \sqrt{1-\mathrm{sech}^2\tilde{z}} = \sqrt{1 - e^{\frac{2C_1}{C_2C_3}\tilde{A}_x}e^{\frac{2}{C_2}\tilde{A}_y}},$$

into equation (3), we arrive at

$$P_{zz}(\tilde{A}_x, \tilde{A}_y) = P_T - \frac{B_0^2}{2\mu_0}\left\{C_1^2 + C_3^2 + 2C_1C_2\left(1 - e^{\frac{C_1-C_2}{C_2C_3}\tilde{A}_x}e^{\frac{1}{C_2}\tilde{A}_y}\right) + C_2^2\left[k\left(1 - e^{\frac{C_1-C_2}{C_2C_3}\tilde{A}_x}e^{\frac{1}{C_2}\tilde{A}_y}\right)^2 + (1-k)\left(1 - e^{\frac{2C_1}{C_2C_3}\tilde{A}_x}e^{\frac{2}{C_2}\tilde{A}_y}\right)\right]\right\}, \tag{7}$$

for k a constant. This form of P_{zz} satisfies $\partial P_{zz}/\partial A_x(\tilde{z}) = 0$ and $\partial P_{zz}/\partial A_y(\tilde{z}) = B_0C_2/(\mu_0 L)\mathrm{sech}^2\tilde{z}$ when $k = C_1/C_2$ and is positive over all (A_x, A_y) when $C_1C_2 < 0$ and $(C_1 - C_2)^2 + C_3^2 < 2\mu_0 P_T/B_0^2$.

Next we use the assumed form of the DF in equation (6) in the definition of the pressure tensor component P_{zz} as the second-order velocity moment of the DF, $P_{zz} = \sum_s m_s \int v_z^2 f_s d^3v$. Note that the pressure tensor should be written as the second-order moment of f_s by $\boldsymbol{w}_s^2 = (\boldsymbol{v} - \boldsymbol{V}_s)^2$, but the DF (equation (6)) is an even function of v_z, which implies that $V_{zs} = 0$. When the dependence of f_s on the Hamiltonian, H_s, is given by $\exp(-\beta_s H_s)$ as it is here, the integral equation for P_{zz} can be interpreted [*Allanson et al.*, 2016] as a Weierstrass transform [e.g., see *Bilodeau*, 1962] and can be amenable to solution by Fourier transforms [e.g., see *Harrison and Neukirch*, 2009a; *Abraham-Shrauner*, 2013], or expansion of g_s in Hermite polynomials [e.g., see *Abraham-Shrauner*, 1968; *Hewett et al.*, 1976; *Channell*, 1976; *Suzuki and Shigeyama*, 2008; *Allanson et al.*, 2015, 2016]. However, using standard integral formulae and/or the fact that exponential functions are eigenfunctions of the Weierstrass transform [e.g. ,see *Wolf*, 1977], we pose the following DF as a solution:

$$f_s\left(H_s, p_{xs}, p_{ys}\right) = \frac{n_{0s}}{\left(\sqrt{2\pi}v_{th,s}\right)^3}e^{-\beta_s H_s} \times \left(a_{0s}e^{\beta_s\left(u_{xs}p_{xs}+u_{ys}p_{ys}\right)} + a_{1s}e^{2\beta_s\left(u_{xs}p_{xs}+u_{ys}p_{ys}\right)} + a_{2s}e^{\beta_s\left(v_{xs}p_{xs}+v_{ys}p_{ys}\right)} + b_s\right), \tag{8}$$

for $a_{0s}, a_{1s}, a_{2s}, b_s, u_{xs}, u_{ys}, v_{xs}$, and v_{ys} as yet arbitrary constants, with the "a, b" constants dimensionless, and the "u, v" constants the bulk flows of individual particle populations [e.g., see *Davidson*, 2001; *Schindler*, 2007].

For the full details describing how the microscopic and macroscopic parameters of the equilibrium are related, and how they are fixed, see Appendix A. In particular, note that b_s must satisfy a certain bound in order to guarantee nonnegativity of the DF.

2.2. The Distribution Function is a Sum of Four Maxwellians

The equilibrium DF in equation (8) is written as a function of the constants of motion (H_s, p_{xs}, p_{ys}), which was suitable for constructing an exact equilibrium solution to the Vlasov equation. However, we can write f_s

explicitly as a function over phase space $(z, \boldsymbol{v})$, in a form similar to that in equation (5). The crucial mathematical step is to complete the square in the exponent of equation (8) [e.g., see *Schindler*, 2007], e.g.,

$$e^{-\beta_s(H_s-u_{xs}p_{xs}-u_{ys}p_{ys})} = e^{q_s\beta_s(u_{xs}A_x+u_{ys}A_y)}e^{\left(u_{xs}^2+u_{ys}^2\right)/\left(2v_{th,s}^2\right)} \times e^{-\left[(v_x-u_{xs})^2+(v_y-u_{ys})^2+v_z^2\right]/\left(2v_{th,s}^2\right)}.$$

In this manner the DF can be rewritten as

$$f_s(z,\boldsymbol{v}) = \frac{1}{\left(\sqrt{2\pi}v_{th,s}\right)^3}\left[\mathcal{N}_{0s}(z)e^{-\frac{(\boldsymbol{v}-\boldsymbol{V}_{0s})^2}{2v_{th,s}^2}} + \mathcal{N}_{1s}(z)e^{-\frac{(\boldsymbol{v}-\boldsymbol{V}_{1s})^2}{2v_{th,s}^2}} + \mathcal{N}_{2s}(z)e^{-\frac{(\boldsymbol{v}-\boldsymbol{V}_{2s})^2}{2v_{th,s}^2}} + be^{-\frac{\boldsymbol{v}^2}{2v_{th,s}^2}}\right], \tag{9}$$

for the population density and bulk flow variables ("$\mathcal{N}$, $\boldsymbol{V}$") defined by

$$\mathcal{N}_{0s}(z) = a_0 e^{q_s\beta_s\boldsymbol{A}\cdot\boldsymbol{V}_{0s}} = a_0 e^{-\tilde{z}}\mathrm{sech}\tilde{z},\ \boldsymbol{V}_{0s} = (u_{xs}, u_{ys}, 0), \tag{10}$$

$$\mathcal{N}_{1s}(z) = a_1 e^{q_s\beta_s\boldsymbol{A}\cdot\boldsymbol{V}_{1s}} = a_1 e^{-2\tilde{z}}\mathrm{sech}^2\tilde{z},\ \boldsymbol{V}_{1s} = (2u_{xs}, 2u_{ys}, 0), \tag{11}$$

$$\mathcal{N}_{2s}(z) = a_2 e^{q_s\beta_s\boldsymbol{A}\cdot\boldsymbol{V}_{2s}} = a_2\mathrm{sech}^2\tilde{z},\ \boldsymbol{V}_{2s} = (v_{xs}, v_{ys}, 0), \tag{12}$$

and with a_0, a_1, a_2, and b defined in Appendix A. It is apparent from consideration of the right-hand side of the definitions of the population densities, that $\boldsymbol{N}_{0s}$, $\boldsymbol{N}_{1s}$, and $\boldsymbol{N}_{2s}$ are in fact independent of species. Note that $\mathcal{N}_{0s} \to 2a_0$ and $\mathcal{N}_{1s} \to 4a_1$ as $\tilde{z} \to -\infty$; $\mathcal{N}_{0s} \to 0$ and $\mathcal{N}_{1s} \to 0$ as $\tilde{z} \to \infty$; and $\mathcal{N}_{2s} \to 0$ as $\tilde{z} \to \pm\infty$.

The representation of f_s in equation (9) has the advantages of having a clear physical interpretation, and of being in a form readily implemented into PIC simulations as initial conditions. Despite the fact that each term of f_s as written in equation (9) bears a strong resemblance to $f_{\mathrm{Maxw},s}$ as defined by equation (5), f_s is an exact Vlasov equilibrium DF, whereas $f_{\mathrm{Maxw},s}$ is not.

Since the DF is a sum of shifted Maxwellian functions, it is important to understand if, and when, it is possible for the DF to have multiple maxima in velocity space, and/or anisotropies, and how the velocity-space structure of the DF depends on the asymmetry of the macroscopic AH+G current sheet equilibrium. A full parameter and/or microstability study of the DF is beyond the scope of this paper. However, we show some preliminary results with parameter values that are consistent with asymmetric conditions that could be relevant to PIC modeling of the magnetopause. In Figure 3 we plot the ion DF in $(\tilde{v}_x, \tilde{v}_y)$ space, for different $\tilde{z}$ values, and for two sets of parameters. The left-hand column is self-consistent with the macroscopic *Parameter Set One*, whereas the right-hand column is self-consistent with the same magnetic field but a higher value of $P_T \approx 4.22B_0^2/(2\mu_0)$, such that $n_{\mathrm{sheath}}/n_{\mathrm{sphere}} = 5.4$: now known as *Parameter Set Two*. In Figure 4 we plot the electron DF for *Parameter Set One* (the electron plots for *Parameter Set Two* are qualitatively very similar). In order to plot the DFs, we must choose values of the constant microscopic parameters that appear in the model. In line with some magnetopause current sheet observations [e.g., *Kaufmann and Konradi*, 1973; *Berchem and Russell*, 1982], and current PIC approaches [e.g., *Hesse et al.*, 2013; *Liu and Hesse*, 2016], we set the characteristic values of these (constant) microscopic parameters by

$$n_{0i} = 1, \quad \delta_i = \frac{m_i v_{th,i}}{eB_0 L} = 0.1, \quad T_{0i}/T_{0e} = 5, \quad \tilde{T}_{0i} + \tilde{T}_{0e} = 1.5,$$

for δ_i the ratio of the ion thermal Larmor radius to the current sheet width, and $\tilde{T}_{0s} = k_B T_{0s}/(B_0^2/(\mu_0 m_i n_{0i}))$, i.e., the characteristic temperatures $\left(k_B T_{0s} = m_s v_{th,s}^2\right)$ are normalized using the characteristic ion Alfvén velocity. We also use a realistic mass ratio $m_i/m_e = 1836$. The actual values of the plasma magnetization, temperature, and temperature ratios will of course be position dependent. Note that both the electron and ion DFs are fully determined once the following parameters are given:

$$n_{0i},\ \delta_i,\ T_{0i}/T_{0e},\ \tilde{T}_{0i} + \tilde{T}_{0e},\ m_i/m_e,\ P_T,\ C_1,\ C_2,\ C_3,$$

and hence, the parameter space to investigate is nine dimensional (in principle one could specify a different set of nine parameters, provided that they are independent).

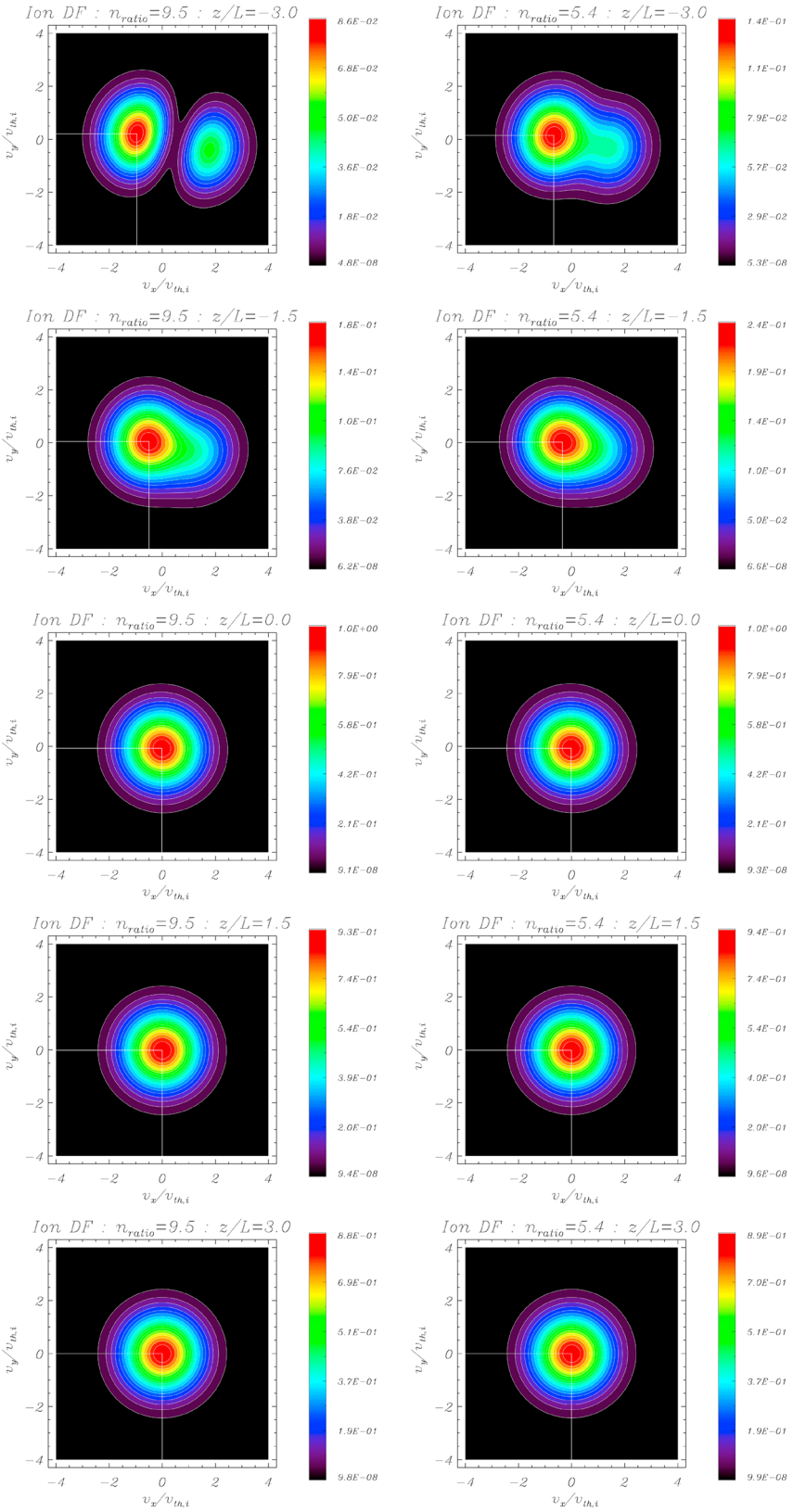

Figure 3. Ion DFs plotted at $\tilde{z} = -3, -1.5, 0, 1.5, 3$ and normalized by $\max_{(v_x,v_y)} f_i(z = 0)$. (left column) Self-consistent with *Parameter Set One*, i.e., $n_{\text{sheath}}/n_{\text{sphere}} = 9.5$. (right column) Self-consistent with *Parameter Set Two*, i.e., $n_{\text{sheath}}/n_{\text{sphere}} = 5.4$.

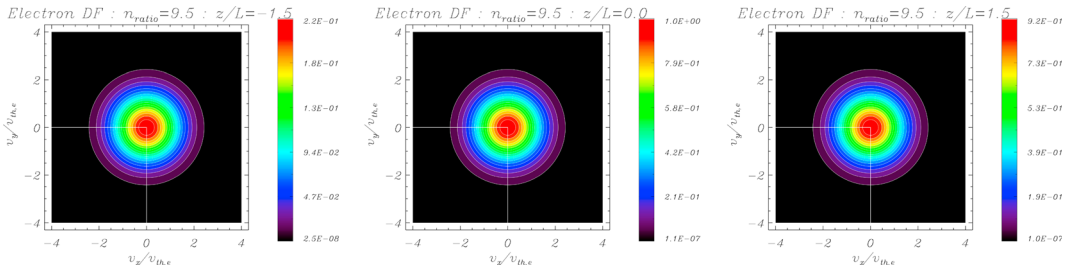

Figure 4. Electron DFs plotted at $\tilde{z} = -1.5, 0, 1.5$ and normalized by $\max_{(v_x,v_y)} f_e(z=0)$. Self-consistent with *Parameter Set One*, i.e., $n_{\text{sheath}}/n_{\text{sphere}} = 9.5$.

By contrasting Figures 3 and 4, we see immediately that is the ions that carry the "non-Maxwellian" features (anisotropies and possibly multiple peaks) for these parameter values. The ion DFs relevant to *Parameter Set One* seem to suggest that stronger macroscopic asymmetries across the current sheet can be self-consistent with more strongly non-Maxwellian ion DFs. Whereas those relevant to *Parameter Set Two* demonstrate that it is possible to construct DFs with single maxima in velocity space, while still maintaining significant asymmetries across the sheet. However, we note that we only present preliminary results here, and a more detailed parameter study will be important to carry out. It may be the case that the ion DFs for *Parameter Set One* are physically unrealistic equilibrium configurations, as they seem susceptible to velocity-space instabilities [*Gary*, 2005] (although the magnitude of the secondary peaks at $\tilde{z} = -3$ are less than 10% of the maximum at $\tilde{z} = 0$), whereas those in *Parameter Set Two* may be more realistic. It will be interesting to carry out analytical and/or numerical stability studies in the future.

In Figure 5 we plot the ion and electron number densities: $n_s(z, \boldsymbol{v}) = \int f_s d^3v$, bulk flows: $\boldsymbol{V}_s(z, \boldsymbol{v}) = n_s^{-1} \int \boldsymbol{v} f_s d^3v$, and kinetic temperatures: $T_s(z) = \left(3k_B n_s\right)^{-1} (P_{xx} + P_{yy} + P_{zz})$, for *Parameter Set One* (the plots for *Parameter Set Two* are qualitatively similar). The number densities are normalized by the n_{0s} parameter; the x and y components of the bulk flow are normalized by $|V_{x,0s} + V_{x,1s} + V_{x,2s}|/3$ and $|V_{y,0s} + V_{y,1s} + V_{y,2s}|/3$ respectively, and the temperatures are normalized by the characteristic ion Alfvén velocity. These curves demonstrate that it is possible for the DF to be self-consistent with strong density, bulk velocity, and kinetic temperature asymmetries across the current sheet. We also see that while the DF is not only self-consistent with $j_x = 0$, it is also consistent with $\boldsymbol{V}_{xs} = 0$; i.e., the independent species bulk flows in the x direction are zero. Furthermore the bulk flows in the y direction decay to zero far from the sheet, in contrast to the aforementioned solution put

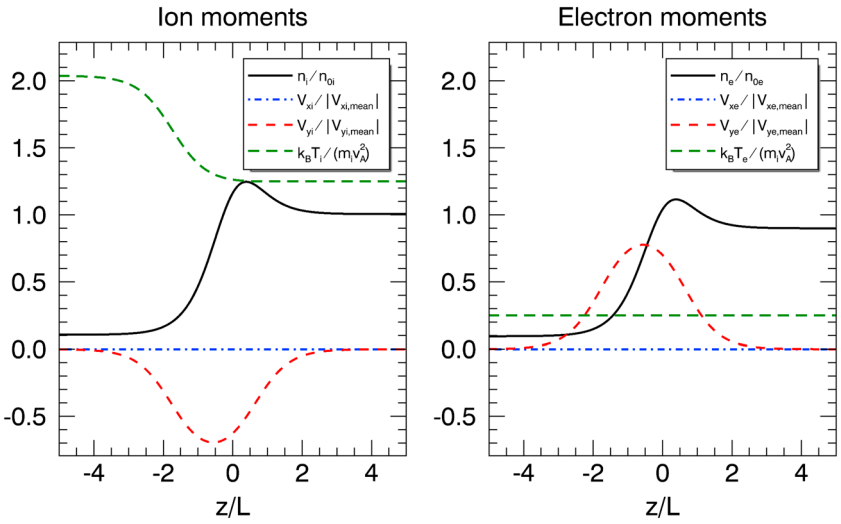

Figure 5. The ion and electron number densities, bulk flows, and temperatures. The number densities, n_s, are normalized by the n_{0s} parameter. The components of the bulk flows, $\boldsymbol{V}_s$, are normalized by the magnitude of the components of $\boldsymbol{V}_{0s} + \boldsymbol{V}_{1s} + \boldsymbol{V}_{2s}/3$. The temperatures are normalized using the characteristic ion Alfvén velocity, $v_{A0} = B_0/\sqrt{\mu_0 m_i n_{0i}}$. Parameter values: *Parameter Set One*.

forward by *Alpers* [1969]. Hence, our solution has bulk flow properties at the boundaries that are consistent with those of the initial conditions of typical PIC simulations of asymmetric reconnection.

3. Discussion

We have presented new, exact and fully self-consistent equilibrium solutions of the Vlasov-Maxwell system in one spatial dimension. Macroscopically, these solutions describe an "asymmetric Harris sheet" magnetic field profile, with finite guide field, such as has often been used in studies of magnetopause current sheets. The expression for the Vlasov equilibrium distribution function is elementary in form and is written as a sum of four exponential functions of the constants of motion, which can be rewritten in $(z, \boldsymbol{v})$ space as a weighted sum of "shifted-Maxwellian" distribution functions. This form for the distribution function can be readily used as initial conditions in particle-in-cell simulations and should be particularly suited to studying asymmetric reconnection processes, with potential relevance to, e.g., Earth's magnetopause. The DF is self-consistent with asymmetric profiles of the magnetic field, kinetic temperature, number density, and dynamic pressure.

Setting up a current sheet that has an exact Vlasov equilibrium in numerical simulations could be helpful for the study of the collisionless tearing instability, which could be important to understand the nature of intense current sheets at the reconnection X line. Oblique tearing modes were recently argued to play a potential role in determining the orientation of the three-dimensional reconnection X line in asymmetric geometry [*Liu et al.*, 2015] and in causing the bifurcated electron diffusion region in the symmetric geometry [*Liu et al.*, 2013]. The former study is especially crucial for predicting the location of magnetic reconnection at Earth's magnetopause under diverse solar wind conditions [*Komar et al.*, 2015]. Such an equilibrium solution also facilitates the study of tearing instabilities under the influence of cross-sheet gradients [*Zakharov and Rogers*, 1992; *Kobayashi et al.*, 2014; *Pueschel et al.*, 2015; *Liu and Hesse*, 2016], important to the onset and suppression of sawtooth crashes in fusion devices.

It will be important in the future to further analyze the velocity-space structure of the DF derived in this paper, how it depends on the microscopic and macroscopic parameters, and the degree of asymmetry across the current sheet. Also, it will be interesting further work to investigate the practical improvement in a PIC simulation of implementing the DF derived in this paper, as compared to the typical fluid-based equilibrium approach.

Appendix A: Equilibrium Parameters and Their Relationships

We now proceed with the necessary task of ensuring that $n_i(A_x, A_y) = n_e(A_x, A_y)$ (for $n_s(A_x, A_y)$ the number density of species s) in order to be consistent with our assumption that $\phi = 0$. The constants a_0, a_1, a_2, and b are defined by these neutrality relations, are found by calculating the zeroth order moment of the DF, and are given by

$$a_0 = n_{0s} a_{0s} e^{\left(u_{xs}^2 + u_{ys}^2\right)/\left(2v_{th,s}^2\right)}, a_2 = n_{0s} a_{2s} e^{\left(v_{xs}^2 + v_{ys}^2\right)/\left(2v_{th,s}^2\right)}, \tag{A1}$$

$$a_1 = n_{0s} a_{1s} e^{2\left(u_{xs}^2 + u_{ys}^2\right)/v_{th,s}^2}, b = n_{0s} b_s. \tag{A2}$$

Note that equations (A1) and (A2) hold for both ions and electrons ($s = i, e$). We must also ensure that the DF in equation (8) exactly reproduces the correct pressure tensor expression of equation (7). After some algebra, we find the "microscopic-macroscopic" consistency relations by taking the v_z^2 moment of the DF, which complete this final step of the method, and are given by

$$P_T - \frac{B_0^2}{2\mu_0}\left[(C_1 + C_2)^2 + C_3^2\right] = b\frac{\beta_e + \beta_i}{\beta_e \beta_i}, \frac{C_1 - C_2}{C_2 C_3 B_0 L} = e\beta_i u_{xi} = -e\beta_e u_{xe}, \tag{A3}$$

$$4C_1 C_2 \frac{B_0^2}{2\mu_0} = a_0 \frac{\beta_e + \beta_i}{\beta_e \beta_i}, \frac{1}{C_2 B_0 L} = e\beta_i u_{yi} = -e\beta_e u_{ye}, \tag{A4}$$

$$-C_1 C_2 \frac{B_0^2}{2\mu_0} = a_1 \frac{\beta_e + \beta_i}{\beta_e \beta_i}, \frac{2C_1}{C_2 C_3 B_0 L} = e\beta_i v_{xi} = -e\beta_e v_{xe}, \tag{A5}$$

$$C_2(C_2 - C_1)\frac{B_0^2}{2\mu_0} = a_2 \frac{\beta_e + \beta_i}{\beta_e \beta_i}, \frac{2}{C_2 B_0 L} = e\beta_i v_{yi} = -e\beta_e v_{ye}. \tag{A6}$$

A1. Nonnegativity of the DF

Since we integrate f_s over velocity space to calculate P_{zz}, it is clear that nonnegativity of P_{zz} does not imply nonnegativity of f_s. Furthermore, it is clear from equations (A1) and (A4) that $C_1 C_2 < 0$ implies that $a_{0s} < 0$ (as well as $a_{1s} > 0$, $a_{2s} > 0$). By completing the square, the DF can be rewritten and we see that nonnegativity of the DF is assured provided $b_s \geq a_{0s}^2/(4a_{1s})$.

Acknowledgments

The authors gratefully acknowledge the support of the Science and Technology Facilities Council Consolidated grant ST/K000950/1 and ST/N000609/1 (O.A., T.N., J.D.B.H., and F.W.), the Science and Technology Facilities Council Doctoral Training grant ST/K502327/1 (O.A. and J.D.B.H), the Natural Environment Research Council grant NE/P017274/1 (Rad-Sat) (O.A.), the NASA grant NNX16AG75G (Y.-H.L), and NASA's Magnetospheric Multiscale Mission (Y.-H.L.). O.A., and F.W. would also like to thank the National Science Foundation for support toward attendance at the AGU Chapman Conference on Currents in Geospace and Beyond, 2016. O.A. would also like to thank the Royal Astronomical Society for a travel grant, for support of attendance at the AGU Fall Meeting 2016. No significant data sets, models, or modeling techniques have been used by—or newly generated by—the authors for use in this paper. Figures 1 and 3–5 have all been constructed using standard mathematical functions and basic IDL plotting routines. All of the information that is necessary to reproduce these figures are included in the manuscript. The authors would like to thank the referees, whose comments have helped to improve the manuscript.

References

Abraham-Shrauner, B. (1968), Exact, stationary wave solutions of the nonlinear vlasov equation, *Phys. Fluids*, *11*, 1162–1167, doi:10.1063/1.1692077.

Abraham-Shrauner, B. (2013), Force-free Jacobian equilibria for Vlasov-Maxwell plasmas, *Phys. Plasmas*, *20*(10), 102117, doi:10.1063/1.4826502.

Allanson, O., T. Neukirch, F. Wilson, and S. Troscheit (2015), An exact collisionless equilibrium for the Force-Free Harris Sheet with low plasma beta, *Phys. Plasmas*, *22*(10), 102116, doi:10.1063/1.4934611.

Allanson, O., T. Neukirch, S. Troscheit, and F. Wilson (2016), From one-dimensional fields to Vlasov equilibria: Theory and application of Hermite polynomials, *J. Plasma Phys.*, *82*(3), 905820306, doi:10.1017/S0022377816000519.

Alpers, W. (1969), Steady State Charge Neutral Models of the Magnetopause, *Astrophys. Space Sci.*, *5*, 425–437, doi:10.1007/BF00652391.

Aunai, N., M. Hesse, S. Zenitani, M. Kuznetsova, C. Black, R. Evans, and R. Smets (2013), Comparison between hybrid and fully kinetic models of asymmetric magnetic reconnection: Coplanar and guide field configurations, *Phys. Plasmas*, *20*(2), 22902, doi:10.1063/1.4792250.

Belmont, G., N. Aunai, and R. Smets (2012), Kinetic equilibrium for an asymmetric tangential layer, *Phys. Plasmas*, *19*(2), 22108, doi:10.1063/1.3685707.

Berchem, J., and C. T. Russell (1982), The thickness of the magnetopause current layer: ISEE 1 and 2 observations, *J. Geophys. Res.*, *87*(A4), 2108–2114, doi:10.1029/JA087iA04p02108.

Bilodeau, G. G. (1962), The Weierstrass transform and Hermite polynomials, *Duke Math. J.*, *29*(2), 293–308, doi:10.1215/S0012-7094-62-02929-0.

Birn, J., and M. Hesse (2010), Energy release and transfer in guide field reconnection, *Phys. Plasmas*, *17*(1), 12109, doi:10.1063/1.3299388.

Burch, J. L., et al. (2016), Electron-scale measurements of magnetic reconnection in space, *Science*, *352*, aaf2939, doi:10.1126/science.aaf2939.

Cassak, P. A., and M. A. Shay (2007), Scaling of asymmetric magnetic reconnection: General theory and collisional simulations, *Phys. Plasmas*, *14*(10), 102114, doi:10.1063/1.2795630.

Channell, P. J. (1976), Exact Vlasov-Maxwell equilibria with sheared magnetic fields, *Phys. Fluids*, *19*, 1541–1545.

Dargent, J., N. Aunai, G. Belmont, N. Dorville, B. Lavraud, and M. Hesse (2016), Full particle-in-cell simulations of kinetic equilibria and the role of the initial current sheet on steady asymmetric magnetic reconnection, *J. Plasma Phys.*, *82*(3), 905820305, doi:10.1017/S002237781600057X.

Davidson, R. C. (2001), *Physics of Nonneutral Plasmas*, Imperial College Press/World Sci., London, U. K.

Dorville, N., G. Belmont, N. Aunai, J. Dargent, and L. Rezeau (2015), Asymmetric kinetic equilibria: Generalization of the BAS model for rotating magnetic profile and non-zero electric field, *Phys. Plasmas*, *22*(9), 92904, doi:10.1063/1.4930210.

Dungey, J. W. (1961), Interplanetary Magnetic Field and the Auroral Zones, *Phys. Rev. Lett.*, *6*, 47–48, doi:10.1103/PhysRevLett.6.47.

Fu, W.-Z., and L.-N. Hau (2005), Vlasov-Maxwell equilibrium solutions for Harris sheet magnetic field with Kappa velocity distribution, *Phys. Plasmas*, *12*(7), 70701, doi:10.1063/1.1941047.

Gary, S. (2005), *Theory of Space Plasma Microinstabilities*, Cambridge Atmos. and Space Sci. Ser., Cambridge Univ. Press.

Gosling, J. T., S. Eriksson, R. M. Skoug, D. J. McComas, and R. J. Forsyth (2006), Petschek-type reconnection exhausts in the solar wind well beyond 1 AU: Ulysses, *Astrophys. J.*, *644*, 613–621, doi:10.1086/503544.

Hapgood, M. A. (1992), Space physics coordinate transformations—A user guide, *Planet. Space Sci.*, *40*, 711–717, doi:10.1016/0032-0633(92)90012-D.

Harris, E. G. (1962), On a plasma sheath separating regions of oppositely directed magnetic field, *Nuovo Cimento*, *23*, 115–121.

Harrison, M. G., and T. Neukirch (2009a), One-dimensional Vlasov-Maxwell equilibrium for the force-free Harris sheet, *Phys. Rev. Lett.*, *102*(13), 135003, doi:10.1103/PhysRevLett.102.135003.

Harrison, M. G., and T. Neukirch (2009b), Some remarks on one-dimensional force-free Vlasov-Maxwell equilibria, *Phys. Plasmas*, *16*(2), 22106, doi:10.1063/1.3077307.

Hesse, M., N. Aunai, S. Zenitani, M. Kuznetsova, and J. Birn (2013), Aspects of collisionless magnetic reconnection in asymmetric systems, *Phys. Plasmas*, *20*(6), 61210, doi:10.1063/1.4811467.

Hesse, M., N. Aunai, D. Sibeck, and J. Birn (2014), On the electron diffusion region in planar, asymmetric, systems, *Geophys. Res. Lett.*, *41*, 8673–8680, doi:10.1002/2014GL061586.

Hesse, M., N. Aunai, J. Birn, P. Cassak, R. E. Denton, J. F. Drake, T. Gombosi, M. Hoshino, W. Matthaeus, D. Sibeck, and S. Zenitani (2016), Theory and modeling for the magnetospheric multiscale mission, *Space Sci. Rev.*, *199*(1), 577–630, doi:10.1007/s11214-014-0078-y.

Hewett, D. W., C. W. Nielson, and D. Winske (1976), Vlasov confinement equilibria in one dimension, *Phys. Fluids*, *19*, 443–449, doi:10.1063/1.861472.

Hoh, F. C. (1966), Stability of sheet pinch, *Phys. Fluids*, *9*, 277–284, doi:10.1063/1.1761670.

Huang, J., Z. W. Ma, and D. Li (2008), Debye-length scaled structure of perpendicular electric field in collisionless magnetic reconnection, *Geophys. Res. Lett.*, *35*, L10105, doi:10.1029/2008GL033751.

Jeans, J. H. (1915), On the theory of star-streaming and the structure of the universe, *Mon. Not. R. Astron. Soc.*, *76*, 70–84, doi:10.1093/mnras/76.2.70.

Kadomtsev, B. B. (1975), Disruptive instability in Tokamaks, *Soviet J. Plasma Phys.*, *1*, 710–715.

Karimabadi, H., V. Roytershteyn, W. Daughton, and Y.-H. Liu (2013), Recent evolution in the theory of magnetic reconnection and its connection with turbulence, *Space Sci. Rev.*, *178*, 307–323, doi:10.1007/s11214-013-0021-7.

Kaufmann, R. L., and A. Konradi (1973), Speed and thickness of the magnetopause, *J. Geophys. Res.*, *78*(28), 6549–6568, doi:10.1029/JA078i028p06549.

Kobayashi, S., B. N. Rogers, and R. Numata (2014), Gyrokinetic simulations of collisionless reconnection in turbulent non-uniform plasmas, *Phys. Plasmas*, *21*(4), 40704, doi:10.1063/1.4873703.

Kolotkov, D. Y., I. Y. Vasko, and V. M. Nakariakov (2015), Kinetic model of force-free current sheets with non-uniform temperature, *Phys. Plasmas*, *22*(11), 112902, doi:10.1063/1.4935488.

Komar, C. M., R. L. Fermo, and P. A. Cassak (2015), Comparative analysis of dayside magnetic reconnection models in global magnetosphere simulations, *J. Geophys. Res. Space Physics*, *120*, 276–294, doi:10.1002/2014JA020587.
Linton, M. G. (2006), Reconnection of nonidentical flux tubes, *J. Geophys. Res.*, *111*, A12S09, doi:10.1029/2006JA011891.
Liu, Y.-H., and M. Hesse (2016), Suppression of collisionless magnetic reconnection in asymmetric current sheets, *Phys. Plasmas*, *23*(6), 60704, doi:10.1063/1.4954818.
Liu, Y.-H., W. Daughton, H. Karimabadi, H. Li, and V. Roytershteyn (2013), Bifurcated structure of the electron diffusion region in three-dimensional magnetic reconnection, *Phys. Rev. Lett.*, *110*(26), 265004, doi:10.1103/PhysRevLett.110.265004.
Liu, Y.-H., M. Hesse, and M. Kuznetsova (2015), Orientation of X lines in asymmetric magnetic reconnection—Mass ratio dependency, *J. Geophys. Res. Space Physics*, *120*, 7331–7341, doi:10.1002/2015JA021324.
Lynden-Bell, D. (1962), Stellar dynamics: Exact solution of the self-gravitation equation, *Mon. Not. R. Astron. Soc.*, *123*, 447.
Malakit, K., M. A. Shay, P. A. Cassak, and C. Bard (2010), Scaling of asymmetric magnetic reconnection: Kinetic particle-in-cell simulations, *J. Geophys. Res.*, *115*, A10223, doi:10.1029/2010JA015452.
Mottez, F. (2003), Exact nonlinear analytic Vlasov-Maxwell tangential equilibria with arbitrary density and temperature profiles, *Phys. Plasmas*, *10*, 2501–2508, doi:10.1063/1.1573639.
Murphy, N. A., M. P. Miralles, C. L. Pope, J. C. Raymond, H. D. Winter, K. K. Reeves, D. B. Seaton, A. A. van Ballegooijen, and J. Lin (2012), Asymmetric magnetic reconnection in solar flare and coronal mass ejection current sheets, *Astrophys. J.*, *751*, 56, doi:10.1088/0004-637X/751/1/56.
Mynick, H. E., W. M. Sharp, and A. N. Kaufman (1979), Realistic Vlasov slab equilibria with magnetic shear, *Phys. Fluids*, *22*, 1478–1484.
Øieroset, M., T. D. Phan, and M. Fujimoto (2004), Wind observations of asymmetric magnetic reconnection in the distant magnetotail, *Geophys. Res. Lett.*, *31*, L12801, doi:10.1029/2004GL019958.
Parker, E. N. (1994), *Spontaneous Current Sheets in Magnetic Fields: With Applications to Stellar X-Rays, Spontaneous Current Sheets in Magnetic Fields*, Int. Ser. in Astron. and Astrophys., vol. 1, Oxford Univ. Press, New York.
Phan, T. D., and G. Paschmann (1996), Low-latitude dayside magnetopause and boundary layer for high magnetic shear: 1. Structure and motion, *J. Geophys. Res.*, *101*, 7801–7816, doi:10.1029/95JA03752.
Phan, T. D., M. A. Shay, J. T. Gosling, M. Fujimoto, J. F. Drake, G. Paschmann, M. Oieroset, J. P. Eastwood, and V. Angelopoulos (2013), Electron bulk heating in magnetic reconnection at Earth's magnetopause: Dependence on the inflow Alfvén speed and magnetic shear, *Geophys. Res. Lett.*, *40*, 4475–4480, doi:10.1002/grl.50917.
Poynting, J. H. (1884), On the transfer of energy in the electromagnetic field, *Philos. Trans. R. Soc.*, *175*, 343–361, doi:10.1098/rstl.1884.0016.
Pritchett, P. L. (2008), Collisionless magnetic reconnection in an asymmetric current sheet, *J. Geophys. Res.*, *113*, A06210, doi:10.1029/2007JA012930.
Pueschel, M. J., P. W. Terry, D. Told, and F. Jenko (2015), Enhanced magnetic reconnection in the presence of pressure gradients, *Phys. Plasmas*, *22*(6), 62105, doi:10.1063/1.4922064.
Quest, K. B., and F. V. Coroniti (1981), Tearing at the dayside magnetopause, *J. Geophys. Res.*, *86*, 3289–3298, doi:10.1029/JA086iA05p03289.
Roytershteyn, V., W. Daughton, H. Karimabadi, and F. S. Mozer (2012), Influence of the lower-hybrid drift instability on magnetic reconnection in asymmetric configurations, *Phys. Rev. Lett.*, *108*(18), 185001, doi:10.1103/PhysRevLett.108.185001.
Schindler, K. (2007), *Physics of Space Plasma Activity*, Cambridge Univ. Press, Cambridge, U. K.
Servidio, S., W. H. Matthaeus, M. A. Shay, P. A. Cassak, and P. Dmitruk (2009), Magnetic reconnection in two-dimensional magnetohydrodynamic turbulence, *Phys. Rev. Lett.*, *102*(11), 115003, doi:10.1103/PhysRevLett.102.115003.
Stark, C. R., and T. Neukirch (2012), Collisionless distribution function for the relativistic force-free Harris sheet, *Phys. Plasmas*, *19*(1), 12115, doi:10.1063/1.3677268.
Suzuki, A., and T. Shigeyama (2008), A novel method to construct stationary solutions of the Vlasov-Maxwell system, *Phys. Plasmas*, *15*(4), 42107, doi:10.1063/1.2908355.
Swisdak, M., B. N. Rogers, J. F. Drake, and M. A. Shay (2003), Diamagnetic suppression of component magnetic reconnection at the magnetopause, *J. Geophys. Res.*, *108*, 1218, doi:10.1029/2002JA009726.
Trenchi, L., M. F. Marcucci, and R. C. Fear (2015), The effect of diamagnetic drift on motion of the dayside magnetopause reconnection line, *Geophys. Res. Lett.*, *42*, 6129–6136, doi:10.1002/2015GL065213.
Wang, P.-R., C. Huang, Q.-M. Lu, and S. Wang (2013), Numerical simulations of magnetic reconnection in an asymmetric current sheet, *Chin. Phys. Lett.*, *30*(12), 125202.
Wilson, F., and T. Neukirch (2011), A family of one-dimensional Vlasov-Maxwell equilibria for the force-free Harris sheet, *Phys. Plasmas*, *18*(8), 82108, doi:10.1063/1.3623740.
Wolf, K. B. (1977), On self-reciprocal functions under a class of integral transforms, *J. Math. Phys.*, *18*(5), 1046–1051.
Zakharov, L., and B. Rogers (1992), Two-fluid magnetohydrodynamic description of the internal kink mode in tokamaks, *Phys. Fluids B*, *4*, 3285–3301, doi:10.1063/1.860384.
Zenitani, S., M. Hesse, A. Klimas, and M. Kuznetsova (2011), New measure of the dissipation region in collisionless magnetic reconnection, *Phys. Rev. Lett.*, *106*(19), 195003, doi:10.1103/PhysRevLett.106.195003.
Zhu, C., R. Liu, D. Alexander, X. Sun, and R. T. J. McAteer (2015), Complex flare dynamics initiated by a filament-filament interaction, *Astrophys. J.*, *813*, 60, doi:10.1088/0004-637X/813/1/60.